Research Square

Preprints are preliminary reports that have not undergone peer review.
They should not be considered conclusive, used to inform clinical practice,
or referenced by the media as validated information.

Protective effects of Qinglongyi-Buguzhi herb pair against H 2 O 2 -induced oxidative injury in B16F10 mouse melanoma cells via PI3K/Akt/Nrf2 signaling pathway

Lele Chen
Shandong University of Traditional Chinese Medicine
Shuguang Chen
Shandong University of Traditional Chinese Medicine
Peng Sun
Shandong University of Traditional Chinese Medicine
Xinyue Liu
Shandong University of Traditional Chinese Medicine
Zhaoshuang Zhan
Shandong University of Traditional Chinese Medicine
Jiafeng Wang (wjfeng2000@126.com)
Shandong University of Traditional Chinese Medicine

Research Article

Keywords: Qinglongyi (the exocarp of Juglans regia L.), Buguzhi (the fruit of Psoralea corylifolia L.), Vitiligo, B16F10 mouse melanoma cells, Oxidative stress injury, PI3K/Akt/Nrf2 signaling pathway

Posted Date: August 5th, 2023

DOI: https://doi.org/10.21203/rs.3.rs-3218065/v1

License: This work is licensed under a Creative Commons Attribution 4.0 International License. Read Full License

Abstract

The herbal pair of Qinglongyi (Q, the exocarp of *Juglans regia* L.)-Buguzhi (B, the fruit of *Psoralea corylifolia* L.) (QB) is commonly used for treating vitiligo in traditional Chinese medicine (TCM). However, the relevant mechanism of QB in the treatment of vitiligo is still unclear. This study aimed to investigate the protective role and mechanism of QB on B16F10 mouse melanoma cells after H_2O_2-induced oxidative stress injury. Firstly, 17 experimental groups were designed as follows: normal control group, H_2O_2 group, Q, B, and QB (mass ratio 1:1, 1:2 and 2:1) low, middle and high concentration groups. MTT was used to detect cell survival rate and flow cytometry was used to determine the content of reactive oxygen species (ROS). Superoxide dismutase (SOD), catalase (CAT) and melanin levels were evaluated using corresponding commercial kits. Based on all the results, the drug group with the best effect was selected for follow-up mechanism study. Then, six experimental groups were designed as follows: normal control group, H_2O_2 group, LY294002 (PI3K inhibitor) group, QB LY294002 group, positive control VE group. Flow cytometry was used to detect cell apoptosis and ROS content. The nuclear translocation of Nrf2 was analyzed using immunofluorescence. RT-qPCR was used to determine the changes in the expression of Akt, Nrf2 and HO-1 genes. Western blot was used to detect the expression of Akt, phospho-Akt (p-Akt), total nuclear factor erythroid 2-related factor 2 (Nrf2), nuclear Nrf2 and heme oxygenase-1 (HO-1) proteins. From our findings, Q, B and QB (1:1, 1:2, 2:1) groups all increased cell survival rate, decreased ROS level and cell apoptosis, upregulated SOD and CAT activity, and increased melanin content of B16F10 cells with H_2O_2 injury. It was worth noting that the QB (1:2) 0.08 mg/mL group had the most prominent effect among all drug groups, so we chosed this group to study the mechanism of action. From the results, when compared with H_2O_2, LY294002, QB LY294002 groups, QB pretreatment of cells in QB group significantly decreased ROS level and apoptosis rate of B16F10 cells with H_2O_2 injury. Moreover, QB up-regulated Akt, Nrf2, HO-1 mRNA expression level and increased p-Akt, HO-1, nuclear Nrf2 proteins expression level, and promoted the nuclear translocation of Nrf2. Notably, LY294002 could largely block the effect of QB. This study demonstrated that QB reversed H_2O_2-induced oxidative stress injury of melanocytes may be related to the activation of PI3K/Akt/Nrf2 signaling pathway.

Introduction

Vitiligo is an acquired chronic skin pigmentation loss disease caused by loss of melanocyte function or a decrease in the number of cells and is mainly characterised by white patches on the skin or mucous membrane areas [1]. Although vitiligo does not cause direct physical damage, it can cause considerable psychosocial distress and impairment of quality of life [2], affecting approximately 0.5%-2.0% of the global population [3]. The current treatment methods for vitiligo mainly include glucocorticoid, calcineurin inhibitors, Vitamin D analogues, prostaglandin analogues and phototherapy [4]. However, existing therapies, although effective in the short term, and can cause numerous adverse reactions and the disease is prone to recurrence. Therefore, we ne ed to develop new effective treatments, and traditional Chinese medicine with definite efficacy and few side effects is the new trend for effective treatment of vitiligo.

As we all know, the complexity of Chinese medicine compounding makes the modernization and development of TCM face many difficulties. The Chinese herbal pair is the most basic and simple one in the compound formula, which is of great significance in the research of Chinese medicine compatibility [5]. Qinglongyi and Buguzhi are traditional Chinese herbs with a long history of application and. “Chinese Materia Medica” ( ) records: Qinglongyi is the dried exocarp of the immature fruit of *Juglans regia* L., and is commonly used to treat cough, carbuncle, ringworm, alopecia areata and vitiligo. According to the Chinese Pharmacopoeia ( ) (2020 version), Buguzhi derives from the dry ripe fruit of *Psoralea corylifolia* L., and has the treatment of kidney-yang deficiency, enuresis and urinary frequency, chills and pain of the waist and kness, alopecia areata, vitiligo. The combination of Qinglongyi and Buguzhi is commonly used in clinical treatment of vitiligo [6, 7]. The clinical applications show that compared with the single preparation of Qinglongyi or Buguzhi, the combination of Qinglongyi and Buguzhi has better therapeutic effect in the treatment of vitiligot, meanwhile with precise efficacy and few adverse reactions [8], but the relevant mechanism has so far not been studied. Recent studies have found that both Qinglongyi and Buguzhi have antioxidant effects and can protect many kinds of cells such as glomerular podocytes [9], nerve cells [10] and human immortalized epidermal cells [11] from oxidative stress. However, it is not clear whether they can improve the oxidative stress damage of melanocytes.

The exact pathogenesis of vitiligo is still unclear, which results in patients not being treated effectively. In recent years, numerous studies have confirmed the important role of OS as an initiator and driver in the vitiligo process. OS leads to the accumulation of ROS in melanocytes and mediates melanocyte dysfunction or death [12, 13]. The PI3K/Akt signaling pathway is a classical pathway involved in a variety of processes, including cell proliferation, migration, apoptosis, and oxidation [14]. Nrf2 is a key factor in the regulation of oxidative stress in cells. Under normal physiological conditions, Nrf2 binds to kelch-like ECH-associated protein-1 (Keap1) and exists in the cytoplasm without biological function [15]. However, under oxidative stress, Nrf2 separates from Keap1, and translocates to the nucleus and binds to the antioxidant response element ARE [16], initiates the transcription of a series of downstream antioxidant genes and phase II detoxification enzymes, such as CAT, SOD, HO-1 and NADPH quinone oxidoreductase-1 (NQO-1) [17]. Previous studies have shown that PI3K/Akt acts as an upstream signal to regulate the activity of Nrf2, enabling the translocation of Nrf2 from cytoplasm to nucleus and enhancing endogenous antioxidant effects [18]. Therefore, activation of the PI3K/Akt/Nrf2 signaling pathway may be an effective strategy for the treatment of vitiligo.

To investigate the protective effects and underlying mechanisms of QB on vitiligo, in this study, we carried out a series of experiments to explore the effect of QB on B16F10 cells after H_2O_2 injury through PI3K/Akt/Nrf2 signaling pathway, in order to provide new ideas for the future research of vitiligo.

Materials and Methods

Main chemicals and reagents

RPMI-1640 medium (C11885500BT) and 100 U/mL penicillin and 100 U/mL strepto-Mycin were acquired from Gibco (Grand Island, NY, USA).Vitamin E (V8011) and MTT (M8180) were purchased from Solarbio (Beijin, China). ROS SOD and CAT kits were acquired from Beyotime Biotechnology (Shanghai, China). Mouse Melanin ELISA kit was purchased from mlbio (Shanghai, China). Cytoplasmic-Nuclear protein extraction kit was acquired from Boster (Wuhan,

China). Bicinchoninic acid (BCA) protein quantification kit and PI3K inhibitor LY294002 were obtained from Beyotime Biotechnology (Shanghai, China). FITC Annexin V Apoptosis Detection Kit I (556547) was acquired from BD Biosciences (San Jose, USA). PrimeScript™ RT reagent Kit with gDNA Eraser (Perfect Real Time) (RR047A) and TB Green® Premix Ex Taq™ II (Tli RNaseH Plus) (RR820A) were purchased from Takara (Osaka City, Osaka Prefecture, Japan). Phospho-Akt (p-Akt, ser473, 4060T), Akt (4691T) and Nrf2 (12721S) were purchased from Cell Signaling Technology (Danvers, MA, USA). HO-1 (ab68477) and Lamin B1 (ab229025) were acquired from Abcam (Cambridge, UK). β-actin (AC026) and FITC goat anti-rabbit IgG (H + L) (AS011) were obtained from Abclonal (Wuhan, China). Goat anti-rabbit IgG-HRP (abs20002) was purchased from absin (Shanghai, China).

Preparation of herbs extracts

Qinglongyi (batch number: 030490102) was purchased from Sanyitang Traditional Chinese Medicine Decoction Pieces Co., Ltd. (Anhui, China), and Buguzhi (batch number: 200501) was obtained from Zhonghe Traditional Chinese Medicine Decoction Pieces Co., Ltd. (Jinan, China). The voucher specimens (Qinglongyi: NO. 20201101; Buguzhi: NO. 20201102) were deposited in the Chinese medicine herbarium of Shandong University of Traditional Chinese Medicine (Jinan, China).

Q and B were separately smashed to a powder. Q (30 g) was extracted with 75% ethanol at reflux for 2 h two times. The ethanol extract was concentrated with a rotary evaporator at 40 ℃ to produce a brown gum. The extraction method of B and QB (mass ratio 1:1, 1:2 and 2:1) was the same as that of Q [8, 19–21]. The extract yields (w/w, dried extract/crude herb) of Q, B, QB (mass ratio 1:1, 1:2 and 2:1) were 10.00%, 12.87%, 14.42%, 9.06%, 11.43%, respectively. The extract was suspended in RPMI-1640 medium to prepare the drug solution of 2mg/ml. Then, the drug solution was filtered by 0.22 μm microporous membrane to remove bacteria, sub-packaged and stored at -20 ℃. Before the experiment, the drug stock solutions were diluted to the desired concentration separately.

Quality control

To ensure the quality of herbs extracts, psoralen, isopsoralen and total flavonoids (calculated by quercetin), which were identified as a chemical marker for quality monitoring, were analyzed by high performance liquid chromatography (HPLC) and ultraviolet-visible spectroscopy (UV-vis), according to the Chinese Pharmacopoeia (2020 version) and Standard of traditional Chinese Medicine in Liaoning Province (Volume 2). The Standard of traditional Chinese Medicine in Liaoning Province (Volume 2) stipulates that the total flavonoids in terms of quercetin ($C_{15}H_{10}O_7$) and dried products should not be less than 0.7% in Qinglongyi, and the Chinese Pharmacopoeia (2020 version) stipulates that the total amount of psoralen ($C_{11}H_6O_3$) and isopsoralen ($C_{11}H_6O_3$) should not be less than 0.70% in terms of dried products in Buguzhi.

Cell culture

B16F10 mouse melanoma cells (CL-0319) were purchased from Procell (Wuhan, China), and cultured in RPMI-1640 medium containing 10% FBS and 1% penicillin-streptomycin. The cultivation conditions were set at 37 ℃, 95% air and 5% CO_2. When cell growth density reached 80–90%, gently removed the original medium. Then added 1 mL trypsin (0.25%) to the culture dish, digested the cells for 1 minute, waited for the cells to become round, added 1mL serum medium to stop digestion. Next, the cells were transferred with a pipette to prepare the cell suspension, and then inhaled into two 1.5 mL centrifuge tubes respectively, and centrifuged at 1000 rpm for 5 minutes. After discarding the supernatant, 1mL culture medium was added to resuspensionand, the cells were finally transferred to two new culture dishes for continuous culture.

Establishment of experimental models

B16F10 cells ($1x10^4$ cells/well) were seeded into 96-well plates and were treated with H_2O_2 solutions at final concentrations of 50, 100, 200, 400 and 600 μM for different times (2 h, 4 h, 6 h, 8 h). MTT was used to detect cell survival rate. An appropriate concentration and time of H_2O_2 was determined to construct a model of oxidative stress injury in B16F10 cells. In this work, 200 μM H_2O_2 for 4 h was chosen to establish the oxidative stress injury model.

Selection of herbs extracts action concentrations

The experimental procedures for screening drug action concentrations were as follows: Firstly, the drug stock solution was diluted to 0.02, 0.04, 0.08, 0.16, 0.32 and 0.64 mg/mL in fresh RPMI1640 medium. Secondly, B16F10 cells ($1x10^4$ cells/well) were inoculated into 96-well plates overnight, and then treated with different concentrations of Q, B, QB (0.02, 0.04, 0.08, 0.16, 0.32 and 0.64 mg/mL) for 24 h. Finally, MTT was used to determine cell survival rate, and then selected the drug concentration which had no significant effect on cell survival rate for follow-up experiments. In this study, 0.02mg/mL, 0.04mg/mL and 0.08mg/mL were selected as action concentrations of Q, B and QB for follow-up experiments.

Evaluation of antioxidation properties of herbs extracts in vitro

Cell grouping

Cells were assigned to 17 groups: normal control group, H_2O_2 group, Q, B, and QB groups. Cells in normal control group were cultured in RPMI-1640 medium. To establish the oxidative injury model, the other 16 groups of cells were treated with a final concentration of 200 μM H_2O_2 solution for 4h. To explore whether Q, B, and QB pretreatment alleviates oxidative injury, B16F10 cells in the Q, B, and QB groups were treated with Q, B, and QB (0.02mg/mL, 0.04mg/mL and 0.08mg/mL) for 24 h before H_2O_2.

Detection of cell survival rate

The MTT method was used to detect the cell survival rate. The cells in logarithmic growth phase were routinely digested, centrifuged and counted. The number of cells was adjusted to $1×10^{-5}$ cells / mL and seeded in 96-well plates with 100 μL per well. Then the culture plates were transferred to 37 ℃ and 5% CO_2 incubator overnight, and added corresponding drugs according to the grouping, zeroing group only added culture medium. During the period of incubation, 20 μL MTT (5 mg/mL) was added to each well and the cells were further incubated for 4 h under the culture conditions. Then, each well added 150 μL DMSO, and

the optical density (OD) at 490 nm was measured using a microplate reader (Bio Tek Cytation 5). Calculating the cell survival rate, cell survival rate (%) = (Experimental group OD-zeroing group OD)/ (normal control group OD-zeroing group OD)× 100%.

ROS detection

The flow cytometry was used to detect ROS level. The cells in logarithmic growth phase were routinely digested, centrifuged and counted. The number of cells was adjusted to 1×10^{-5} cells/mL and seeded in 6-well plates with 2 mL per well, then the culture plates were transferred to 37 ℃ and 5% CO_2 incubator overnight. When the cell growth density reached 60% 70% and added corresponding drugs according to the grouping for 24 h. The culture medium was discarded and the cells were incubated with fresh medium containing 10 mmol/L DCFH-DA for 20 min at 37 ℃, then washed with PBS (pH 7.4) three times. The fluorescence of DCF was measured using a flow cytometer (CytoFLFXS).

Superoxide dismutase (SOD) and catalase (CAT) assays

Collecting the processed cells and after lysis of cells, the protein content was detected by BCA kit, and the activities of superoxide dismutase (SOD) and catalase (CAT) were determined by superoxide SOD and CAT kits, according to the manufacturer's instructions.

Detection of melanin

Collecting the processed cells and after lysis of cells, the melanin content was measured with a ELISA kit, in accordance with the manufacturer's instructions.

Mechanism studies of QB based on PI3K/Akt/Nrf2 signaling pathway

Cell grouping

The cells were divided into 6 groups as follows: normal control group, H_2O_2 group, QB group, LY294002 (PI3K inhibitor) group, QB + LY294002 group and VE group (Vitamin E was chosen as the positive control drug). Cells in normal control group were cultured in RPMI-1640 medium. To establish the oxidative injury model, the other 5 groups of cells were treated with a final concentration of 200 μM H_2O_2 for 4h. To explore whether QB pretreatment alleviates oxidative injury, cells in QB group and QB + LY294002 group were treated with QB (0.08mg/mL) for 24 h before H_2O_2. To investigate whether QB can protect melanocytes from oxidative stress injury through PI3K/Akt/Nrf2 signal pathway, cells in LY294002 group and QB + LY294002 group were preincubated with LY294002 (20 μmol/L) for 2 h before QB.

Detection of ROS

The detection steps were the same as **ROS detection**.

Apoptosis assay

The cells in logarithmic growth phase were routinely digested, centrifuged and counted. The number of cells was adjusted to 1×10^{-5} cells/mL and seeded in 6-well plates with 2 mL per well, then the culture plates were transferred to 37 ℃ and 5% CO_2 incubator overnight. When the cell growth density reached 60% 70% and added corresponding drugs according to the grouping for 24 h. Then, the cells were digested and collected, and washed with cold PBS two times. 300 μL binding buffer was added to resuspended cells and 5 μL FITC Annexin V and PI were added respectively. After reaction for 30 min at room temperature and under dark conditions, the apoptosis rate of cells was detected by flow cytometry.

Reverse transcription-quantitative polymerase chain reaction (RT-qPCR)

The cells that had been processed were collected and the total RNA was isolated using TRIzol® reagent. The RT reaction was performed using PrimeScript™ RT reagent with gDNA Eraser kit, and quantitative real-time PCR reaction was performed with TB Green® Premix ExTaq™ II kit following the manufacturer's instructions. RT-qPCR analyses were performed with the LightCycler® 480 system. β-actin was used as an internal reference, the relative mRNA expression levels of Akt, Nrf2, and HO-1 were quantified using the $2^{-\Delta\Delta Ct}$ method. The Oligonucleotide sequences of specific primers for Akt, Nrf2, and HO-1 as follows:

Gene	Forward primer sequences (5′–3′)	Reverse primer sequences (5′–3′)
Akt	5′-CATCGTGTGGCAGGATGTGTA–3′	5′-ACCTGGTGTCAGTCTCAGAGGTG–3′
Nrf2	5′-GCACATCCAGACAGACACCAG–3′	5′-TATCCAGGGCAAGCGACTCAT–3′
HO-1	5′-CTGGAGATGACACCTGAGGTCAA–3′	5′-CTGACGAAGTGACGCCATCTG–3′
β-actin	5′-CATCCGTAAAGACCTCTATGCCAAC–3′	5′-ATGGAGCCACCGATCCACA–3′

Western blot

The cells that had been processed were collected and lysed with RIPA lysis buffer. Nuclear protein was extracted using the Cytoplasmic-Nuclear protein extraction kit, and protein concentration was determined using a BCA kit. The cells were mixed with 5X loading buffer to denature in boiling water. Each protein sample (30 μg) was subjected to 10% SDS-PAGE, then the separated proteins were transferred into PVDF membranes. After 2 h of blocking with 5% skimmed milk at room temperature, the membranes were incubated at 4 ˚C overnight with primary antibodies against phospho-Akt (1:2000), Akt (1:1000), Nrf2 (1:1000), HO-1 (1:30000), Lamin B1 (1:1000), and *β*-actin (1:50000). *β*-actin and Lamin B1 were used as controls. The next day, the membranes were incubated with

Goat anti-rabbit IgG-HRP (1:5000) for 1.5 h at room temperature. The bound antibodies were visualized using an enhanced chemiluminescence reagent under the multicolor fluorescence imaging system. Then, the gray values of each blot was measured by ImageJ software.

Immunofluorescence staining

The B16F10 cells were seeded on glass slides in a 6-well plates, and treated with the indicated drugs. The cells that had been processed were collected and washed 3 times with PBS and fixed with 4% formaldehyde solution for 30 min, then permeated with 0.3% Triton X-100 for 10 min, and blocked with 5% goat serum for 30 min at 37 ˚C. The cells were then incubated with primary anti-Nrf2 antibody Nrf2 (1:200) overnight at 4 ˚C. Next day, the cells were washed 3 times with PBS and incubated with FITC goat anti-rabbit IgG (H + L)(1:200) for 1 h at 37 ˚C under dark condition, then the cell nuclei were counterstained with DAPI for 5 min. Finally, the nuclear translocation of Nrf2 was observed using fluorescence microscopy.

Statistical analysis

All data were expressed as mean ± standard deviation (SD). SPSS 22.0 software was used for statistical analysis. Two-way ANOVA followed by post hoc Tukey's test was performed to evaluate the antioxidation properties of Q, B, QB, and one-way ANOVA with Tukey's post hoc test was used to analyze other groups differences. $P < 0.05$ was considered to be statistically significant.

Results

Analysis of chemical markers for quality monitoring

The total flavonoids (calculated by quercetin), the chemical markers for quality monitoring of Qinglongyi, were analyzed by UV-vis. Psoralen and isopsoralen, the chemical markers for quality monitoring of Buguzhi, were analyzed by HPLC. The results showed that Qinglongyi calculated in terms of dried products, the content of total flavonoids (calculated by quercetin) was 1.58%, which was much higher than 0.7% stipulated in the standard of traditional Chinese medicine in Liaoning Province (Fig. 1A-C), and Buguzhi calculated in terms of dried products, the total content of psoralen and isopsoralen was 1.1%, which was higher than 0.7% stipulated in Chinese Pharmacopoeia.(Fig. 1D-E), indicating that the herbs used meet the quality standards, and the quality of herbs extracts could be assured.

Appropriate concentration and time of H_2O_2

MTT method was used to determine the cell survival rate. According to the experimental results to select an appropriate concentration and time of H_2O_2, and to construct a model of oxidative stress injury in B16F10 cells. The results showed that with the increase of concentration and time of H_2O_2, the cell survival rate decreased gradually (Fig. 2A and Fig. 2B). Compared with the control group, treatment with 200 μM H_2O_2 for 4 h significantly inhibited cell viability, the cell survival rate was 58.98 ± 2.69% ($P < 0.01$), which was closed to the IC50, this result was stable and reproducible. Therefore, 200 μM H_2O_2 for 4 h was selected to establish the oxidative stress injury model in B16F10 cells.

Concentrations of Q, B and QB

MTT method was used to detect the cell survival rate, and then selected the concentrations of Q, B and QB with no significant effect on cell survival rate. As shown in Fig. 3, compared with the control group, there were no significant changes in cell viability at the concentration range of 0 0.08 mg/mL ($P > 0.05$). Therefore, 0.02, 0.04 and 0.08 mg/mL were selected as the working concentration in the following experiments.

Effects of Q, B, QB on oxidative stress injury in B16F10 cells

Q, B and QB protect B16F10 cells against H_2O_2-induced cell death

MTT method was used to detect the effects of Q, B, QB on the cell survival rate of H_2O_2-induced oxidative stress injury in B16F10 cells. The results as shown in Fig. 4, the cell survival rate was significantly reduced in H_2O_2 group ($P < 0.01$) compared to the control. However, compared with the H_2O_2 group, pretreatment with Q, B, QB for 24 h significantly increased cell survival rate in a dose-dependent manner ($P < 0.01$). These results demonstrated that Q, B, QB could effectively increase the cell survival rate of B16F10 cells to reduce the oxidative stress injury induced by H_2O_2.

Q, B and QB improve the antioxidant capacity of B16F10 cells

ROS, SOD and CAT are indicators of oxidative stress. The results revealed that the H_2O_2 group exhibited higher ROS levels ($P < 0.01$) and lower SOD and CAT activities compared to the control group ($P < 0.01$). After pretreatment with Q, B and QB (Q, B, QB groups), the levels of ROS were significantly ($P < 0.05$) decreased, while the activities of SOD and CAT were obviously increased ($P < 0.05$). In addition, we found that the antioxidant capacity of QB (1:2) and QB (2:1) groups were stronger than other groups, and QB (1:2) (0.08mg/mL) group had the most prominent anti-oxidant effect ($P < 0.05$). These results indicated that Q, B, QB all could improve the anti-oxidant capacity of B16F10 cells against H_2O_2-induced oxidative stress injury, and QB (1:2) (0.08mg/mL) group had the most prominent anti-oxidant effect (Fig. 5A-C).

Q, B and QB promote melanin production of B16F10 cells

Melanin is the main cause of pigmentation in human hair, eyes and skin. Blockage of melanin synthesis pathway can lead to skin diseases such as albinism, halo nevus, and vitiligo [22]. Protecting melanocytes function and promoting melanin production are of great significance to the treatment of vitiligo. Therefore, we determined the content of melanin. The results as shown in Fig. 6, compared with the control group, melanin content was obviously decreased

in the H_2O_2 group ($P < 0.01$), whereas preincubation with Q, B, QB increased the melanin content ($P < 0.01$). Besides, the melanin content of QB (1:2) and QB (2:1) groups were higher than other groups, the QB (1:2) group had higher melanin content than the QB (2:1) group, and the QB (1:2) (0.08mg/mL) group had the highest melanin content ($P < 0.05$).

Summary

The above results suggested that Q, B and QB all had protective effects on H_2O_2-induced oxidative stress injury in B16F10 cells, but QB (1:2) 0.08mg/mL group had the most significant effect, so we selected this group for mechanism studues.

QB reverses H_2O_2-induced oxidative stress injury via regulating PI3K/Akt/Nrf2 signaling pathway in B16F10 cells

QB inhibits H_2O_2-induced ROS production

To investigate the antioxidant function of PI3K/Akt/Nrf2 signaling pathway in QB, we measured the ROS levels. Compared with the control group, the ROS level in H_2O_2 group was significantly increased ($P < 0.01$). However, pretreatment with QB in QB group, the ROS level was effectively decreased compared with the H_2O_2 group ($P < 0.01$), and there was a similar trend in VE group ($P < 0.01$). The PI3K inhibitor LY294002 (LY294002 group) increased the ROS level compared with the QB ($P < 0.01$). While compared with the LY294002 group, the ROS level was decreased again in the QB + LY294002 group ($P < 0.05$). The results as shown in Fig. 7A-B.

QB reverses H_2O_2-induced apoptosis

To explore whether the protective effect of QB was via cell apoptosis, we detected the cell apoptosis rate by flow cytometry. The cell apoptosis rate in H_2O_2 group was obviously increased compared to control group ($P < 0.01$). While compared with the H_2O_2 group, pretreatment with QB and VE (QB group and VE group) significantly decreased the cell apoptosis rate ($P < 0.01$). The inhibition of PI3K in the LY294002 group increased the cell apoptosis rate compared to the QB group ($P < 0.01$). In addition, compared with the LY294002 group, the cell apoptosis rate was also decreased in the QB + LY294002 group, but the difference was not statistically significant ($P > 0.05$) (Fig. 8A-B).

QB promotes the expression of Akt, Nrf2 and HO-1 genes

To investigate the molecular mechanism of QB reducing oxidative stress, we determined whether QB treatment activated the antioxidant pathway of PI3K/Akt/Nrf2, and RT-qPCR was used to detect the expression of relevant genes. The results as shown in Fig. 9A-C, compared with the control group, the expression level of Akt, Nrf2 and HO-1 were increased in H_2O_2 group ($P < 0.01$ or $P < 0.05$). When pretreatment with QB, the expression level of Akt, Nrf2 and HO-1 were significantly increased in the QB group ($P < 0.01$ or $P < 0.05$) compared to the H_2O_2 group. However, the PI3K inhibitor LY294002 partly blocked this increasing expression in LY294002 and QB + LY294002 groups.

QB increases the expression of Akt, Nrf2 and HO-1 proteins

Western blot was used to detect the expression of relevant proteins. The results showed that compared with the control group, the expression level of p-Akt, HO-1 and nuclear Nrf2 were upregulated in H_2O_2 group ($P < 0.01$ or $P < 0.05$). After treatment with QB, the expression level of p-Akt, HO-1 and nuclear Nrf2 were significantly increased in QB group ($P < 0.01$ or $P < 0.05$) compared to the H_2O_2 group. While compared with the QB group, pretreatment with LY294002 obviously decreased the expression of p-Akt, HO-1 and nuclear Nrf2 in LY294002 and QB + LY294002 groups ($P < 0.01$ or $P < 0.05$, Fig. 8A-D). The expression of Akt and total Nrf2 had an increasing trend, but the difference was not statistically significant ($P > 0.05$, Fig. 10E-F).

QB induces the nuclear translocation of Nrf2

Immunofluorescence staining results as shown in Fig. 11A-B. The translocation of Nrf2 was promoted in H_2O_2 group ($P < 0.05$) compared to the control group. When pretreatment with QB (QB group), the translocation of Nrf2 was obviously increased in QB group ($P < 0.01$). While the translocation of Nrf2 was significantly reduced after treatment with PI3K inhibitor LY294002 (LY294002 and QB + LY294002 groups) when compared with QB group ($P < 0.05$).

Summary

The above results indicated that H_2O_2 promoted the activation of the PI3K/Akt/Nrf2 signaling pathway, and QB could further activate PI3K/Akt/Nrf2 signaling pathway to ameliorate H_2O_2-induced oxidative stress injury in B16F10 cells. The mechanism of QB protective effect on H2O2-induced oxidative stress injury in B16F10 mouse melanoma cells was shown in Fig. 12.

Discussion

Vitiligo is a common clinical skin disease with complex pathological mechanisms and difficult treatment, causing great mental stress to patients and seriously affecting their quality of life. Currently, the therapies used to treat vitiligo mainly include corticosteroids, calcineurin inhibitors, vitamin D_3 analogs, phototherapy etc. These treatments are effective in the short term, but they have many adverse effects and high price [23], so new treatment options for vitiligo are urgently needed. Traditional Chinese medicine has the characteristics of obvious curative effect, small side effects and multiple targets and is the new trend for effective treatment of vitiligo.

According to the “Chinese Materia Medica” ( ), Qinglongyi is bitter and astringent in taste, and flat in nature. It has the effect of clearing heat and detoxifying, dispelling wind and healing ringworm, relieving pain and dysentery. “Compendium of Materia Medica” ( ) records: one green walnut peel, a bar of soap-sized sulfur, and grind well. Mix and apply every day to achieve the effect of treating vitiligo. Chinese Pharmacopoeia ( ) (2020 edition) records: Buguzhi is pungent and bitter in taste, and warm in nature, and exhibits actions on the spleen meridian and kidney meridian, and has the functions of reinforcing kidney and strengthening yang, helping inspiration and relieving asthma, warming spleen and stopping diarrha, securing essence and reducing urination, and externally used to treat vitiligo and alopecia areata. As for the compatibility of Qinglongyi and Buguzhi, “Compendium of Materia Medica” ( ) records that the effect of Buguzhi combined with Qinglongyi or Huma is better. Clinical cases show that Qinglongyi and Buguzhi are commonly used in clinical treatment of vitiligo [6, 7], and the combination of the two drugs can improve the efficacy in the treatment of vitiligo [8], but the relevant mechanism has so far not been studied.

Previous studies found that Qinglongyi could upregulate the expression of PI3K protein and gene to protect glomerular foot cells from oxidative stress injury [9]. Buguzhi might exert protective effects against oxidative injury in HaCaT cells via activating the Nrf2 signaling pathway [11]. However, the protective effect of Qinglongyi, Buguzhi or Qinglongyi-Buguzhi on oxidative damage of melanocytes has not been reported. A growing number of studies have shown that oxidative stress plays an important role in the pathogenesis of vitiligo, which can directly lead to damage or complete destruction of functional melanocytes [24, 25]. Many studies found that the levels of ROS, H_2O_2, and MDA were elevated, the lipid peroxidation was enhanced, and the levels of CAT, GSH-Px, SOD were reducedin the skin lesions or serum of patients with vitiligo [26–28], confirming that impaired redox balance is a possible mechanism in vitiligo.

PI3K/Akt signaling pathway plays an important role in reducing apoptosis and increasing cell viability of melanocytes damaged by oxidative stress [29–31]. Nrf2, a transcription factor, plays an important role in regulating the expression of antioxidant enzymes in melanocytes and is a major target for vitiligo treatment [32]. It has been demonstrated that the PI3K/Akt pathway can regulate the expression and activity of Nrf2 and restore cellular oxidation-antioxidation homeostasis [33–35]. B16F10 mouse melanoma cells are highly homologous to human epidermal melanocytes. In addition, B16F10 mouse melanoma cells are easy to obtain and stable for passage, and are one of the most commonly used models for studying pigmentary disorders of the skin [36–38]. H_2O_2 is an endogenous source of cellular oxidative stress and is often used as an inducer to establish a model of cellular oxidative stress injury, and to explore the mechanisms of cellular oxidative injury and the protection of antioxidants against oxidative injury [39, 40].

Based on the above researches, in this study, we prepared the experimental drugs of Q, B and QB (1:1, 1:2, 2:1), and established H_2O_2-induced oxidative stress injury cell model with the B16F10 mouse melanoma cells to investigate the impact of Q, B and QB on oxidative stress, and determine the optimal efficacy group. In addition, to explore the underlying mechanism based on the PI3K/Akt/Nrf2 signaling pathway.

Our study demonstrated that after exposure to 200 μM H_2O_2 for 4 h, B16F10 cells viability was obviously decreased, the level of ROS was remarkably increased, the activities of SOD and CAT were significantly decreased, and the content of melanin was obviously reduced. However, Q, B and QB pretreatment mitigated the H_2O_2-induced increase in ROS, up-regulated cells viability, improved SOD and CAT activities, and increased melanin content. Notably, the QB (1:2) 0.08 mg/mL group had the most significant effect among all groups, implying that Q, B and QB (1:1, 1:2, 2:1) all could alleviate H_2O_2-induced oxidative stress injury response of B16F10 cells and exert antioxidant activity, but the antioxidant capacity of QB (1:2) 0.08 mg/mL group was the strongest. Therefore, QB (1:2) 0.08 mg/mL group was selected to study the relevant mechanisms. We explored the PI3K/Akt/Nrf2 signaling pathway which was closely related to oxidative stress. We found that the ROS level and cell apoptosis were significantly increased, and the expression of Akt, Nrf2 and HO-1 genes were improved, the expression of p-Akt, nuclear Nrf2 and HO-1 proteins were upregulated, and the translocation of Nrf2 was promoted in B16F10 cells with H_2O_2-induced oxidative injury. While QB reduced the level of ROS and cell apoptosis, significantly increased the gene expression levels of Akt, Nrf2, HO-1, obviously upregulated the protein expression levels of p-Akt, nuclear Nrf2, HO-1, and markedly promoted Nrf2 nuclear translocation. However, treatment with the PI3K inhibitor LY294002 could partially reverse the effect of QB pretreatment on increasing the gene expression levels of Akt, Nrf2, HO-1 and the protein expression levels of p-Akt, nuclear Nrf2, HO-1, and the translocation of Nrf2 in B16F10 cells with H_2O_2-induced oxidative injury, implying that QB could reduce the H_2O_2-induced oxidative injury in B16F10 cells via the PI3K/Akt/Nrf2 signaling pathway.

Conclusions

In this study, the B16F10 mouse melanoma cells were used as the research object, the oxidative damage model was established by H_2O_2 to induce, and with QB pretreatment of B16F10 cells during H_2O_2-induced oxidative injury. We found that QB had a significant protective effect on B16F10 cells with H_2O_2-induced oxidative injury, and the protective function was confirmed by a series of experimental data, including the detection of ROS levels, SOD and CAT activities, melanin content, and cell survival rate and apoptosis rate. In addition, the translocation of Nrf2 and the expression of oxidative injury-related proteins such as Akt, Nrf2, HO-1 were detected in subsequent investigation. All the results showed that QB had a significant protective effect on B16F10 cells with H_2O_2-induced oxidative injury via increasing the expression levels of oxidative injury-related proteins. This study revealed that QB could reverse H_2O_2-induced oxidative injury via promoting the activation of PI3K/Akt/Nrf2 signaling pathway in B16F10 cells. Thus, our study provides a direction for the development of new drugs for vitiligo, meanwhile it provides a new target for the prevention and treatment of vitiligo.

Abbreviations

Q, Qinglongyi; B, Buguzhi; QB, Qinglongyi-Buguzhi; OS, oxidative stress; ROS, reactive oxygen species; SOD, superoxide dismutase; CAT, catalase; MTT, 3-(4,5-dimethyl-2-thiazolyl)-2,5-diphenyl-2-H-tetrazolium bromide; ELISA, enzyme-linked immunosorbent assay; RT-qPCR, reverse transcription-quantitative polymerase chain reaction; NQO-1, NADPH quinone oxidoreductase-1; PBS, phosphate buffered saline; VE, Vitamin E; Keap1, kelch-like ECH-associated protein-1; p-Akt, phospho-Akt; Nrf2, nuclear factor erythroid 2-related factor 2; HO-1, heme oxygenase-1; SD, standard deviation.

Declarations

Authors contributions LC and SC conceived and designed the study. PS and XL participated in the experiments. LC wrote and submitted the manuscript. JW and ZZ revised the manuscript. All authors read and approved the final version of manuscript.

Funding This work was supported by Qilu School of Traditional Chinese Medicine Academic School Inheritance Project (Qilu Authentic Chinese medicine processing characteristics of traditional Chinese medicine, Characteristic techniques of traditional Chinese medicine for Fever Differentiation and treatment of Qilu Wen Disease School); Graduate Education Quality Improvement Program of Shandong Province (No. SDYAL20053, No. SDYKC21047).

Conflict of interest The authors declare that they have no competing interests.

References

1. Ezzedine, K., Eleftheriadou, V., Whitton, M., van Geel, N (2015) Vitiligo. Lancet 386(9988): 74-84. https://doi.org/10.1016/S0140-6736(14)60763-7
2. Bergqvist C, Ezzedine K (2020) Vitiligo: A Review. Dermatology 236(6): 571-592. https://doi.org/10.1159/000506103
3. Ongenae K, Van Geel N, De Schepper S, Naeyaert JM (2005) Effect of vitiligo on self-reported health-related quality of life. Br J Dermatol 152(6): 1165-1172. https://doi.org/10.1111/j.1365-2133.2005.06456.x
4. Karagaiah P, Valle Y, Sigova J, Zerbinati N, Vojvodic P, Parsad D, Schwartz RA, Grabbe S, Goldust M, Lotti T (2020) Emerging drugs for the treatment of vitiligo. Expert Opin Emerg Drugs 25(1): 7-24. https://doi.org/10.1080/14728214.2020.1712358
5. Wang S, Hu Y, Tan W, Wu X, Chen R, Cao J, Chen M, Wang Y (2012) Compatibility art of traditional Chinese medicine: from the perspective of herb pairs. J Ethnopharmacol 143(2): 412-423. https://doi.org/10.1016/j.jep.2012.07.033
6. Liu CJ (1989) Observation on the curative effect of traditional Chinese medicine on 46 cases of vitiligo. J Med Theory Pract 2(02): 21. https://kns.cnki.net/kcms2/article/abstract?v=WMl_cnbuli4jgUQFNqDsEff4MUYX7FV8aL8r-rBynQvVrQ-0Kp81SZzRaxseBixWdDPyjmH1A7WPOp9650QnxDhdCzTPzehMumaT16uT5HTuL1U-xc4DgkBADIN93nfz&uniplatform=NZKPT&language=CHS
7. Ding X, Wu XH (2017) Professor Xu Xian's experience in treating vitiligo. Chin J Integr Tradit West Med 37(05): 624-625. https://kns.cnki.net/kcms/detail/11.2787.R.20170428.0553.014.html
8. Zhao RT, Chen XM, Hou XJ (2008) Preparation Technology of Psoralea corylifolia-Juglans regia Tincture. Chin Pharm 19(30): 2349-2350. https://kns.cnki.net/kcms2/article/abstract?v=WMl_cnbuli6RAwjvVZIlwZboDfLAaYFTIx9diMX4SJxff8juIwLl3jIbq2vcTKzRiOFYLEDC9IBF7exPcyCQyouf63pMaD3iHOwrC-wyZyt7jDfGFt4D_PgnVgukT2Dh&uniplatform=NZKPT&language=CHS
9. Liu WW (2021) Effects of Compound Qinglongyi Capsules on expression of CD2AP and PI3K in podocytes of adriamycin nephropathy rats. Heilongjiang University of Traditional Chinese Medicine. https://doi.org/10.27127/d.cnki.ghlzu.2021.000152
10. Guan YH, Hai J (2016) Protection of psoralen on PC-12 cell damage induced by H_2O_2. Drugs & Clinic 31(05): 577-581. https://kns.cnki.net/kcms2/article/abstract?v=WMl_cnbuli55WIC1Qi2xhZzXGE0zgB9c3clt_n8syjS9lOFgmxzdKf3_A3Iwt8qhquZ1iIEvxeNq7B4OsTaUVLTwX9vQONOohTe8tCV9ktI86_3xejWitw3HAlsaH
11. Liu T (2020) Research on the anti-aging effect and mechanism of Corylin and its nanostructured lipid carrierin Psoralea corylifolia Linn. Tianjin University of Traditional Chinese Medicine. https://doi.org/10.27368/d.cnki.gtzyy.2020.000083
12. Xuan Y, Yang Y, Xiang L, Zhang C (2022) The Role of Oxidative Stress in the Pathogenesis of Vitiligo: A Culprit for Melanocyte Death. Oxid Med Cell Longev 2022: 8498472. https://doi.org/10.1155/2022/8498472
13. Chen J, Li S, Li C (2021) Mechanisms of melanocyte death in vitiligo. Med Res Rev 41(2): 1138-1166. https://doi.org/10.1002/med.21754
14. Wang D, Zhou W, Chen J, Wei W (2019) Upstream regulators of phosphoinositide 3-kinase and their role in diseases. J Cell Physiol 234(4): 0021-9541. https://doi.org/10.1002/jcp.28215
15. Keum YS, Choi BY (2014) Molecular and chemical regulation of the Keap1-Nrf2 signaling pathway. Molecules 19(7): 10074-10089. https://doi.org/10.3390/molecules190710074
16. Lu MC, Ji JA, Jiang ZY, You QD (2016) The Keap1-Nrf2-ARE Pathway As a Potential Preventive and Therapeutic Target: An Update. Med Res Rev 36(5): 924-963. https://doi.org/10.1002/med.21396
17. Lee JM, Johnson JA (2004) An important role of Nrf2-ARE pathway in the cellular defense mechanism. J Biochem Mol Biol 37(2): 139-143. https://doi.org/10.5483/bmbrep.2004.37.2.139
18. Chen S, Li X, Wang Y, Mu P, Chen C, Huang P, Liu D (2019) Ginsenoside Rb1 attenuates intestinal ischemia/reperfusion-induced inflammation and oxidative stress via activation of the PI3K/Akt/Nrf2 signaling pathway. Mol Med Rep 19(5): 3633-3641. https://doi.org/10.3892/mmr.2019.10018
19. Li SF, Sun GC. Bao SJ, Zhang N (1997) Study on the toxicity of Juglans regia tincture. J Guiyang Med Coll 22(4): 36-38. https://doi.org/10.19367/j.cnki.1000-2707.1997.04.011

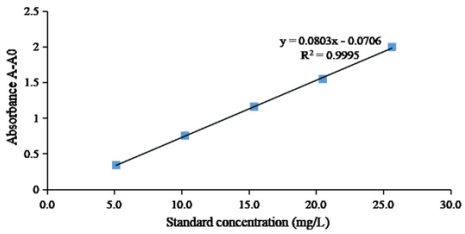
20. Sun DX (2019) The study of Chemical constituents from Diaphragma Juglandis Fructus and Green walnut husks. Jilin Agricultural University. https://doi.org/10.27163/d.cnki.gjlnu.2019.000207
21. Di QF (2019). Study on optimal extraction of Psoralea corylifolia L. Guangdong Chemical Industry 46(23): 45-46. https://kns.cnki.net/kcms2/article/abstract?v=WMl_cnbuli7YaENibRNGQDkGJqXu3nU3S2pnChDwZPKF-3-aVyFb0LGWpUUDk-u2jeDyXfA4laTXzggsohV2ELcvO7EoHEpvdbE3rMNAm5KToscxVD8fV8rfIBouWshVfx_VjEYkLxs=&uniplatform=NZKPT&language=CHS
22. Cordero RJB, Casadevall A (2020) Melanin. Curr Biol 30(4): R142-R143. https://doi.org/10.1016/j.cub.2019.12.042
23. Felsten LM, Alikhan A, Petronic-Rosic V (2011) Vitiligo: a comprehensive overview Part II: treatment options and approach to treatment. J Am Acad Dermatol 65(3): 493-514. https://doi.org/10.1016/j.jaad.2010.10.043
24. Yamamoto A, Yang L, Kuroda Y, Guo J, Teng L, Tsuruta D, Katayama I (2020) Local Epidermal Endocrine Estrogen Protects Human Melanocytes against Oxidative Stress, a Novel Insight into Vitiligo Pathology. Int J Mol Sci 22(1): 269. https://doi.org/10.3390/ijms22010269
25. Denat L, Kadekaro AL, Marrot L, Leachman SA, Abdel-Malek ZA (2014) Melanocytes as instigators and victims of oxidative stress. J Invest Dermatol 134(6): 1512-1518. https://doi.org/10.1038/jid.2014.65
26. Mathachan SR, Khurana A, Gautam RK, Kulhari A, Sharma L, Sardana K (2021) Does oxidative stress correlate with disease activity and severity in vitiligo? An analytical study. J Cosmet Dermatol 20(1): 352-359. https://doi.org/10.1111/jocd.13499
27. Speeckaert R, Dugardin J, Lambert J, Lapeere H, Verhaeghe E, Speeckaert MM, van Geel N (2018) Critical appraisal of the oxidative stress pathway in vitiligo: a systematic review and meta-analysis. J Eur Acad Dermatol Venereol 32(7):1089-1098. https://doi.org/10.1111/jdv.14792
28. Gao XW (2020) Observation of curative effect of treating vitiligo with Milli-fire needle and effect on CAT SOD in venous blood. Urumqi: Xinjiang Medical University. https://doi.org/10.27433/d.cnki.gxyku.2020.000490
29. Lu W, Zhao Y, Kong Y, Zhang W, Ma W, Li W, Wang K (2018) Geniposide prevents H_2O_2-induced oxidative damage in melanocytes by activating the PI3K-Akt signalling pathway. Clin Exp Dermatol 43(6): 667-674. https://doi.org/10.1111/ced.13409
30. Yang B, Yang Q, Yang X, Yan HB, Lu QP (2016) Hyperoside protects human primary melanocytes against H_2O_2-induced oxidative damage. Mol Med Rep 13(6): 4613-4619. https://doi.org/10.3892/mmr.2016.5107
31. Larribere L, Khaled M, Tartare-Deckert S, Busca R, Luciano F, Bille K, Valony G, Eychene A, Auberger P, Ortonne JP, Ballotti R, Bertolotto C (2004) PI3K mediates protection against TRAIL-induced apoptosis in primary human melanocytes. Cell Death Differ 11(10): 1084-1091. https://doi.org/10.1038/sj.cdd.4401475
32. Ko H, Kim MM (2019) H_2O_2promotes the aging process of melanogenesis through modulation of MITF and Nrf2. Mol Biol Rep 46(2): 2461-2471. https://doi.org/10.1007/s11033-019-04708-8
33. Kim H, Park CS, Lee AY (2017) Reduced Nrf2 activation in PI3K phosphorylation-impaired vitiliginous keratinocytes increases susceptibility to ROS-generating chemical-induced apoptosis. Environ Toxicol 32(12): 2481-2491. https://doi.org/10.1002/tox.22461
34. Xiong J, Yang J, Yan K, Guo J (2021) Ginsenoside Rk1 protects human melanocytes from H_2O_2-induced oxidative injury via regulation of the PI3K/AKT/Nrf2/HO-1 pathway. Mol Med Rep 24(5): 821. https://doi.org/10.3892/mmr.2021.12462
35. Sugimoto M, Ko R, Goshima H, Koike A, Shibano M, Fujimori K (2021) Formononetin attenuates H2O2-induced cell death through decreasing ROS level by PI3K/Akt-Nrf2-activated antioxidant gene expression and suppressing MAPK-regulated apoptosis in neuronal SH-SY5Y cells. Neurotoxicology 85: 186-200. https://doi.org/10.1016/j.neuro.2021.05.014
36. Moon SY, Akter KM, Ahn MJ, Kim KD, Yoo J, Lee JH, Lee JH, Hwangbo C (2022) Fraxinol Stimulates Melanogenesis in B16F10 Mouse Melanoma Cells through CREB/MITF Signaling. Molecules 27(5):1549. https://doi.org/10.3390/molecules27051549
37. Wang HM, Qu LQ, Ng JPL, Zeng W, Yu L, Song LL, Wong VKW, Xia CL, Law BYK (2022) Natural Citrus flavanone 5-demethylnobiletin stimulates melanogenesis through the activation of cAMP/CREB pathway in B16F10 cells 98:153941. https://doi.org/10.1016/j.phymed.2022.153941
38. Cho H, Kim B, Kim OS, Kim Y, Yang Y, Song J, Liu D, Jeon S, Kim O (2021) Photochemical reaction to increase melanogenesis using Buddleja officinalis and blue light-emitting diode irradiation in B16F10. Photodiagnosis Photodyn Ther 35:102456. https://doi.org/10.1016/j.pdpdt.2021.102456
39. Wang Z, Wei D, Xiao H (2013) Methods of cellular senescence induction using oxidative stress. Methods Mol Biol 1048: 135-144. https://doi.org/10.1007/978-1-62703-556-9_11
40. Li M, Zhang Y, Han T, Guan L, Fan D, Wu Q, Liu J, Xu Y, Fan Y (2023) Verniciflavanol A, a profisetinidin-type-4-arylflavan-3-ol from toxicodendron vernicifluum protects SH-SY5Y cells against H_2O_2-induced oxidative stress. Phytochemistry 205:113487. https://doi.org/10.1016/j.phytochem.2022.113487

Figures

A

Standard concentration (mg/L)	Absorbance A	A-A0
5.1	0.697	0.343
10.2	1.111	0.757
15.4	1.516	1.162
20.5	1.905	1.551
25.6	2.356	2.002

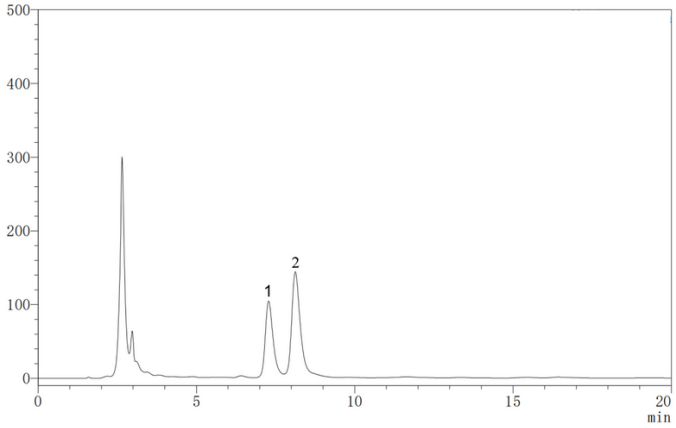
B



C

Tested substance	Sample weight m (g)	Constant volume V (mL)	Dilution ratio f	Absorbance A	A-A0	Measured concentration C (mg/L)	Content X (%)	Average value (%)
Total flavonoids (calculated by quercetin)	2.0082	100	33.3	0.973	0.619	8.59	1.57	1.58
	2.0875	100	33.3	1.012	0.658	9.07	1.59	

D



E

Tested substance	Sample weight m	Measured concentration C	Content in the samples X1	Total amount of psoralen and isopsoralen in samples	Average value
	g	mg/L	%	%	%
Psoralen	0.5051	16.825	0.44	1.10	1.10
Isopsoralen		27.954	0.66		
Psoralen	0.5020	16.661	0.44	1.10	
Isopsoralen		27.729	0.66		

Figure 1

The total flavonoids (calculated by quercetin), the chemical markers for quality monitoring of Qinglongyi, were analyzed by UV-vis. Psoralen and isopsoralen, the chemical markers for quality monitoring of Buguzhi, were analyzed by HPLC. **A** The table of standard concentration and absorbance, **B**standard curve, **C** the content of total flavonoids (calculated by quercetin), **D** chromatogram: 1 psoralen, 2 isopsoralen, **E** the total content of psoralen and isopsoralen.

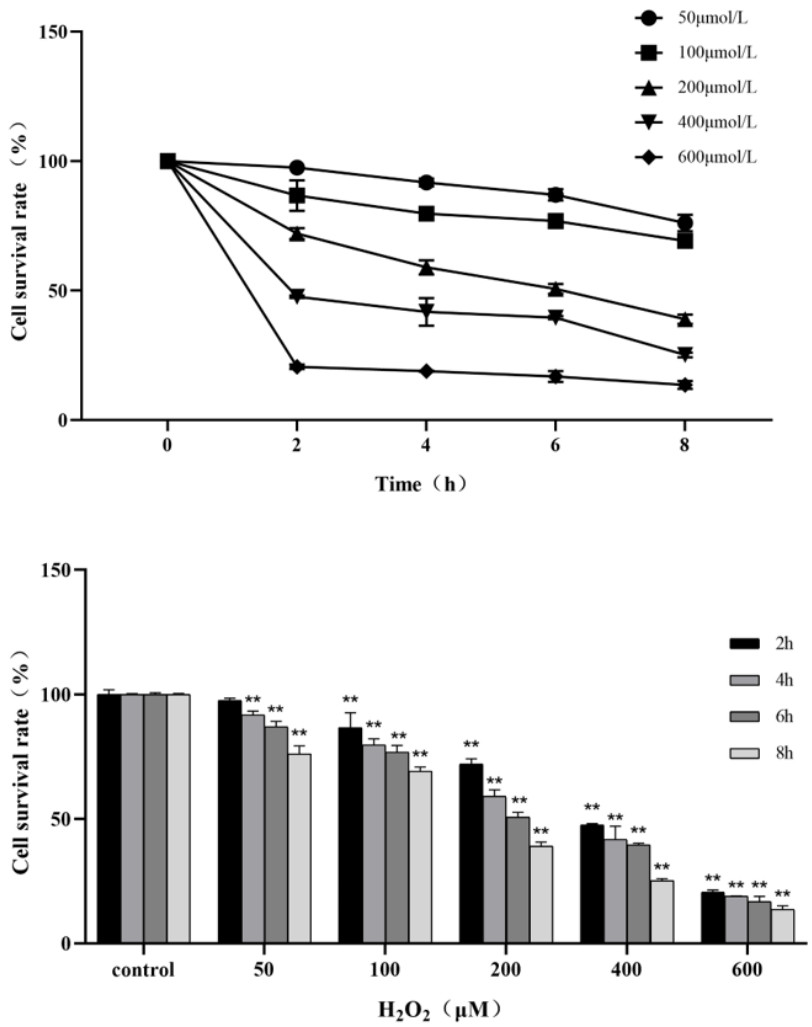


Figure 2

An appropriate concentration and time of H_2O_2 was determined to construct a model of oxidative stress injury in B16F10 cells. MTT was used to detect cell survival rate. **A** The effect of H_2O_2 was in a concentration-dependent manner. **B** The effect of H_2O_2 was in a time-dependent manner. When compared with the control group, the significance was $^{*}P < 0.05$, $^{**}P < 0.01$. All data are expressed as mean±SD, n=3 for each group.

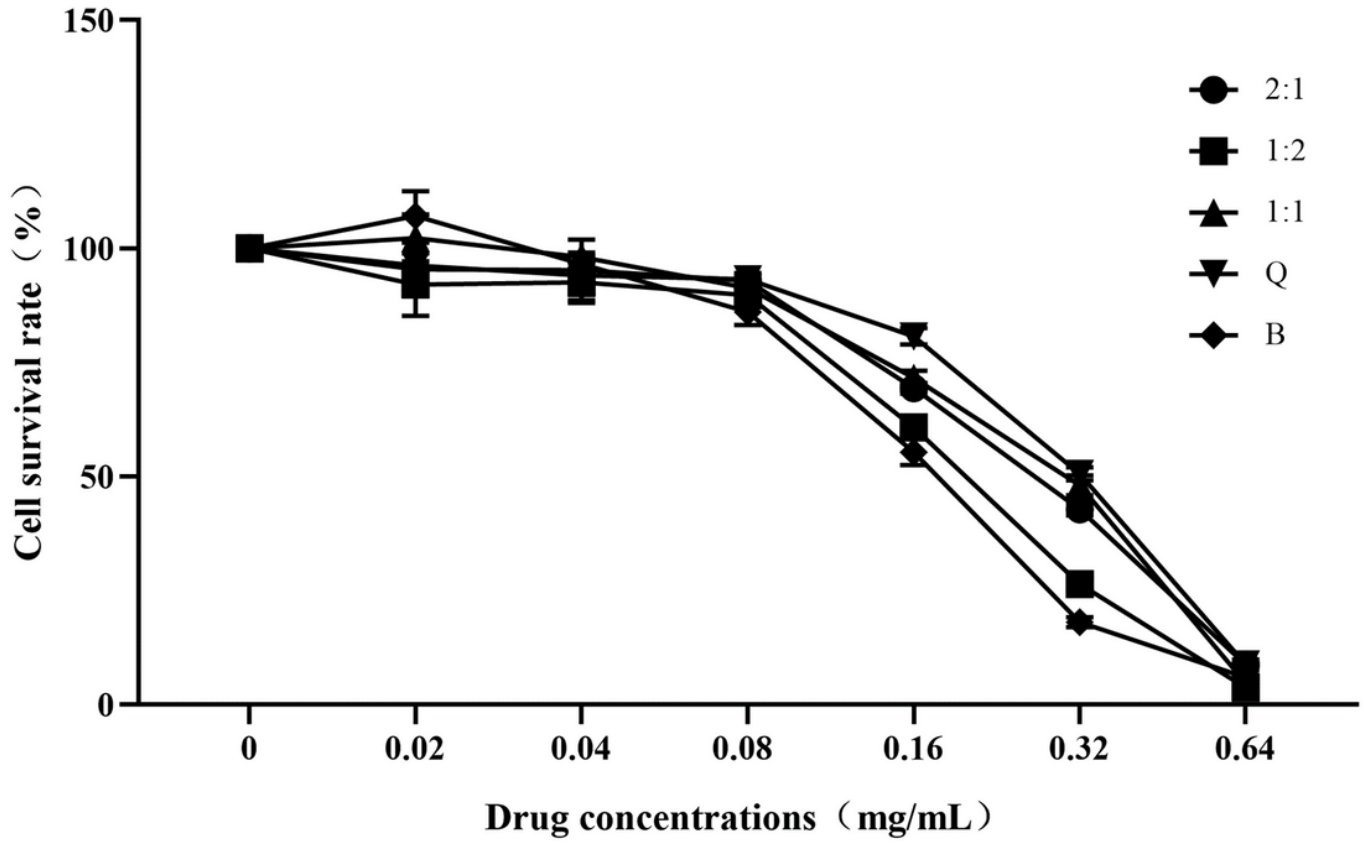


Figure 3

An appropriate action concentration of Q, B and QB were selected. MTT was used to detect cell survival rate, and then selected the drug concentration which had no significan t effect on cell survival rate for follow-up experiments. When compared with the control group, the significance was $^{*}P < 0.05$, $^{**}P < 0.01$. All data are expressed as mean±SD, n=3 for each group.

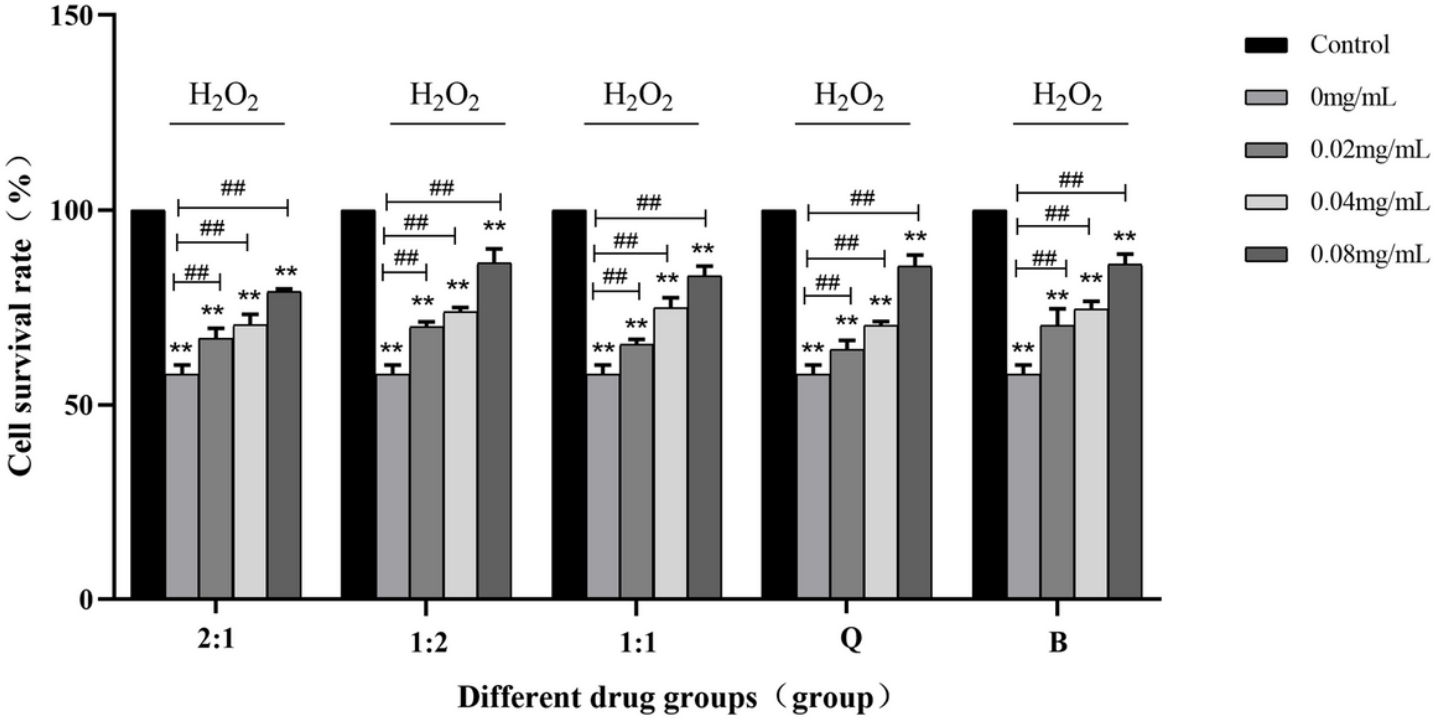


Figure 4

An appropriate action concentration of Q, B and QB were selected. MTT was used to detect cell survival rate, and then selected the drug concentration which had no significant effect on cell survival rate for follow-up experiments. When compared with the control group, the significance was $^{*}P < 0.05$, $^{**}P < 0.01$; when compared with the H_2O_2 group, the significance was $^{\#}P < 0.05$, $^{\#\#}P < 0.01$. All data are expressed as mean±SD, n=3 for each group.

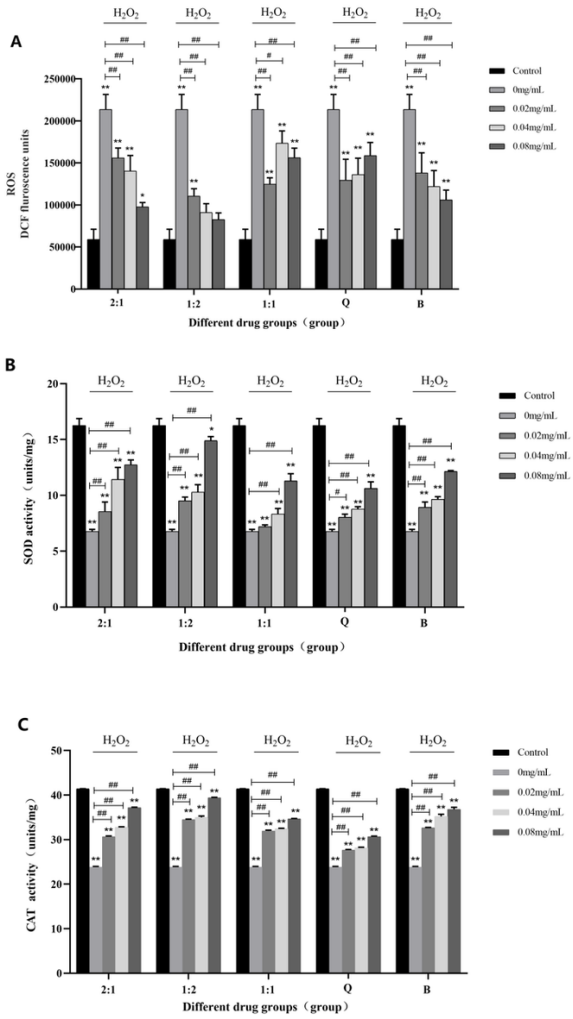


Figure 5

Effects of Q, B and QB (1:1, 1:2, 2:1) on oxidative stress response in B16F10 mouse melanoma cells. **A** ROS, **B** SOD and **C** CAT activities in B16F10 cells. When compared with the control group, the significance was $^{*}P < 0.05$, $^{**}P < 0.01$; when compared with the H_2O_2 group, the significance was $^{\#}P < 0.05$, $^{\#\#}P < 0.01$. All data are expressed as mean±SD, n=3 for each group.

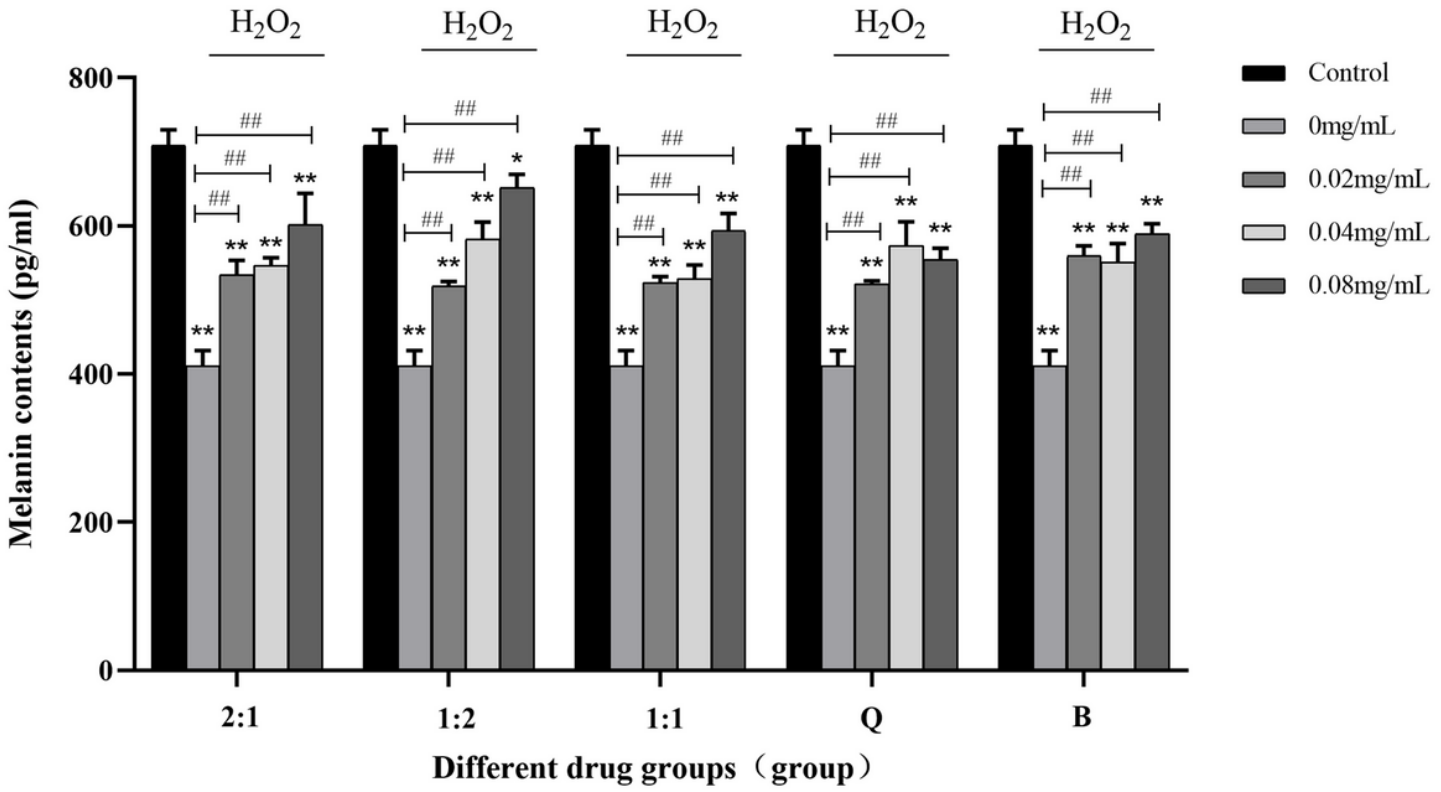


Figure 6

Effects of Q, B and QB (1:1, 1:2, 2:1) on melanin contents in B16F10 mouse melanoma cells. The melanin content was measured using ELISA method. When compared with the control group, the significance was $^{*}P < 0.05$, $^{**}P < 0.01$; when compared with the H_2O_2 group, the significance was $^{\#}P < 0.05$, $^{\#\#}P < 0.01$. All data are expressed as mean±SD, n=3 for each group.

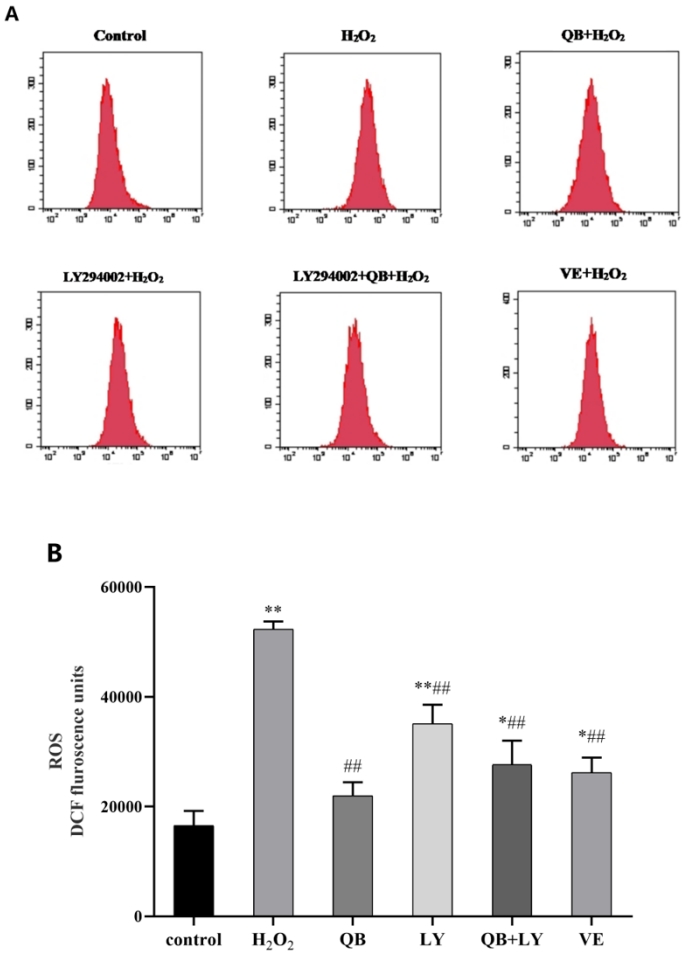


Figure 7

Effects of QB on ROS levels in B16F10 mouse melanoma cells. **A** The representative images of DCF fluorescence. **B** The ROS levels of the B16F10 cells in different treatment groups. When compared with the control group, the significance was $^{*}P < 0.05$, $^{**}P < 0.01$; when compared with the H_2O_2 group, the significance was $^{\#}P < 0.05$, $^{\#\#}P < 0.01$. All data are expressed as mean±SD, n=3 for each group.

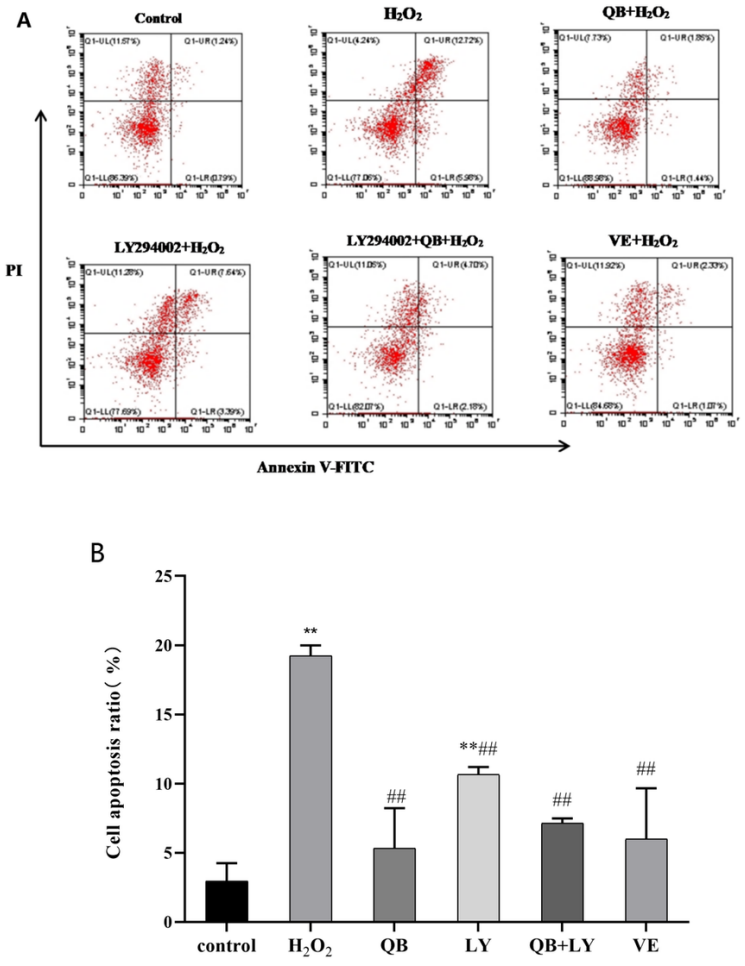


Figure 8

Effects of QB on cell apoptosis in B16F10 mouse melanoma cells. **A** Representative images of flow cytometry. **B** The apoptosis of the B16F10 cells in different treatment groups. When compared with the control group, the significance was $^{*}P < 0.05$, $^{**}P < 0.01$; when compared with the H_2O_2 group, the significance was $^{\#}P < 0.05$, $^{\#\#}P < 0.01$. All data are expressed as mean±SD, n=3 for each group.

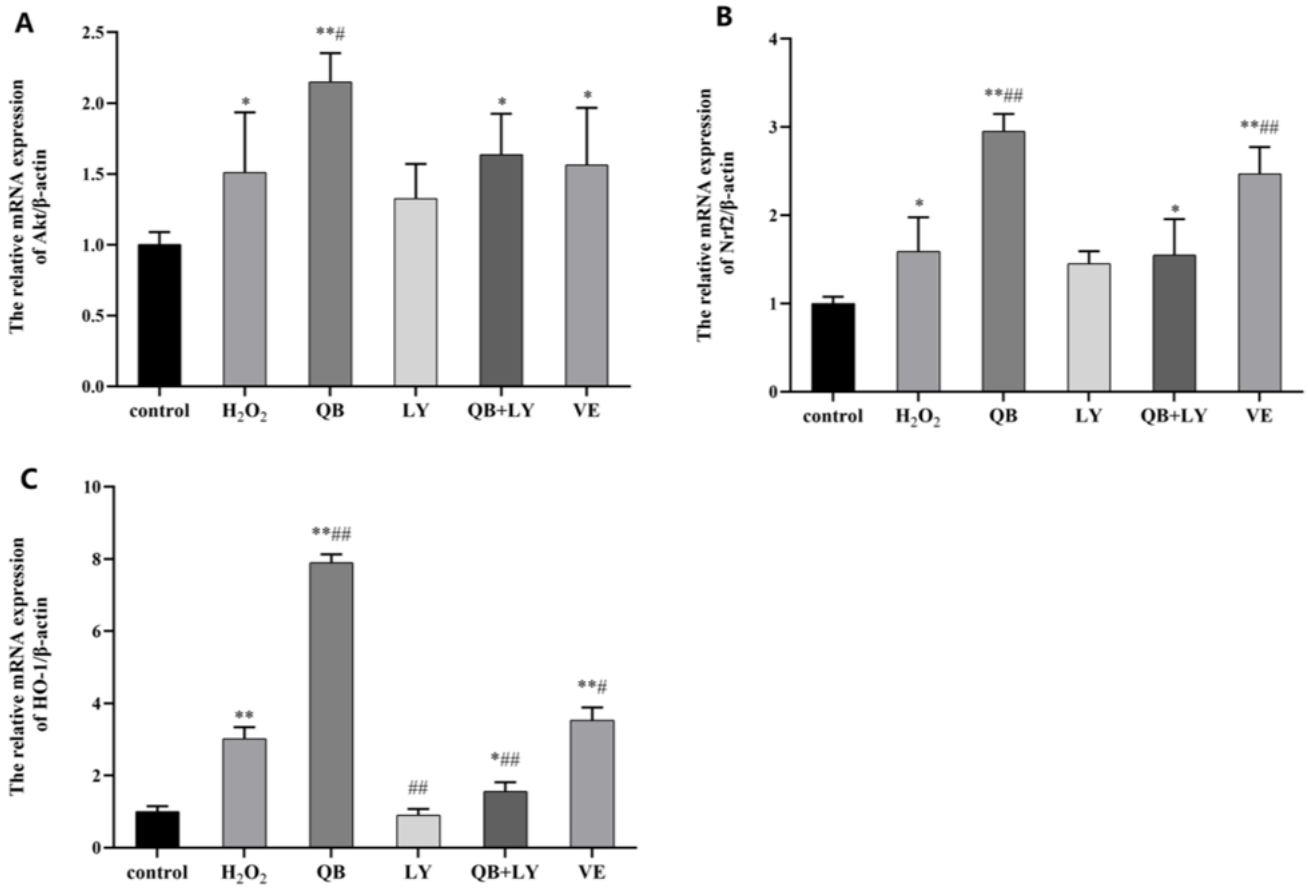


Figure 9

Effects of QB on the expression of Akt, Nrf2 and HO-1 genes in B16F10 mouse melanoma cells. The mRNA expression levels of Akt, Nrf2, HO-1 was determined by RT-qPCR. **A** Akt, **B** Nrf2, **C** HO-1 the relative mRNA expression levels in B16F10 cells with H_2O_2-induced oxidative stress injury under different treatments. β-actin was used as an internal reference. When compared with the control group, the significance was $^{*}P < 0.05$, $^{**}P < 0.01$; when compared with the H_2O_2 group, the significance was $^{\#}P < 0.05$, $^{\#\#}P < 0.01$. All data are expressed as mean±SD, n=3 for each group.

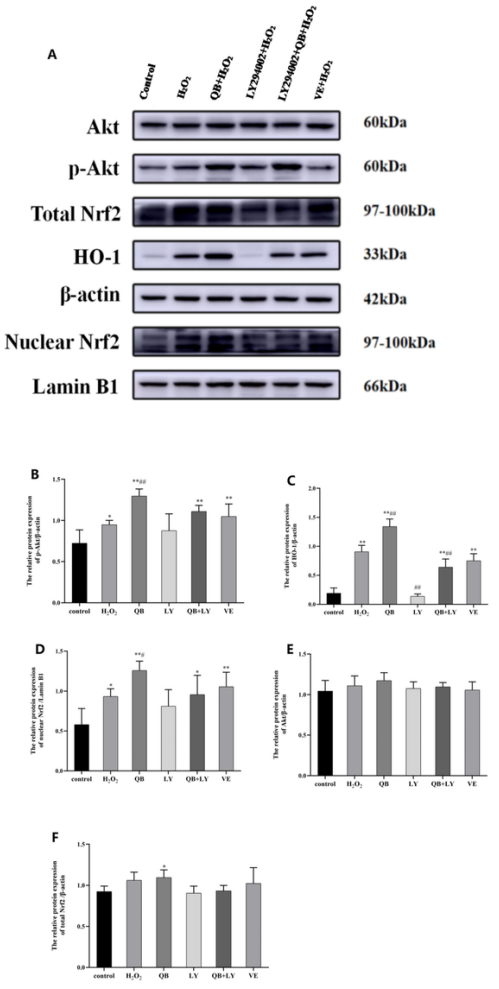


Figure 10

Effects of QB on the expression of Akt, p-Akt, total Nrf2, nuclear Nrf2 and HO-1 proteins in B16F10 mouse melanoma cells. The relative protein expression levels of Akt, p-Akt, total Nrf2, nuclear Nrf2 and HO-1 was detected by western blot. **A** results of the related proteins expressions, **B** p-Akt, **C** HO-1, **D** nuclear Nrf2, **E** Akt, **F** total Nrf2 the relative protein expression levels in B16F10 cells with H_2O_2-induced oxidative stress injury under different treatments. β-actin and Lamin B1 were used as an internal reference. When compared with the control group, the significance was $^{*}P < 0.05$, $^{**}P < 0.01$; when compared with the H_2O_2 group, the significance was $^{\#}P < 0.05$, $^{\#\#}P < 0.01$. All data are expressed as mean±SD, n=3 for each group.

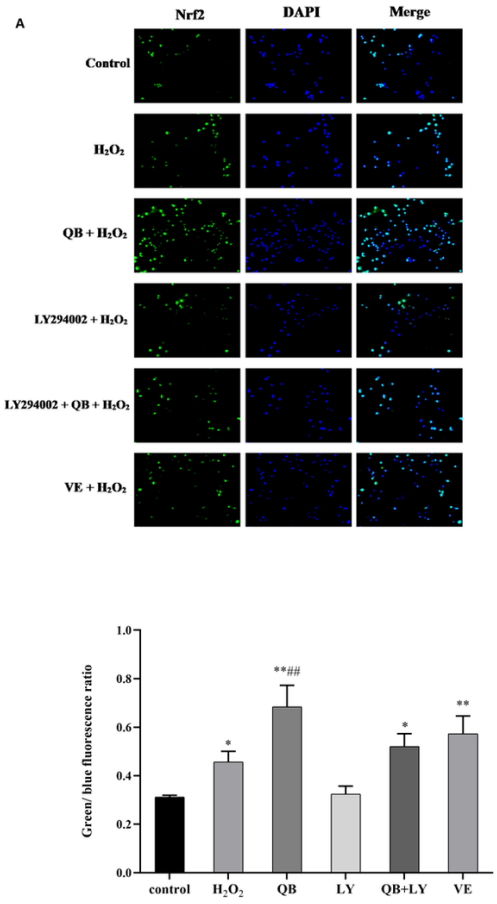


Figure 11

Effects of QB on the nuclear translocation of Nrf2 in B16F10 mouse melanoma cells. Immunofluorescence staining method was used to measure the nuclear translocation of Nrf2. **A** the representative images of immunofluorescence staining, **B** the results of the nuclear translocation of Nrf2 in B16F10 cells with H_2O_2-induced oxidative stress injury under different treatments. When compared with the control group, the significance was $^{*}P < 0.05$, $^{**}P < 0.01$; when compared with the H_2O_2 group, the significance was $^{\#}P < 0.05$, $^{\#\#}P < 0.01$. All data are expressed as mean±SD, n=3 for each group.